BMC Cancer

RESEARCH Open Access

A novel prognostic model utilizing TMTV and SUVmax from ^{18}F-FDG PET/CT for predicting overall survival in patients with extranodal NK/T- cell lymphoma

Hua Wang[1*†], Demei Feng[1†], Yiwen Mo[1†], Huangming Hong[2†], Yingying Hu[1], Li Huang[3], Xiaolei Wei[4], Yajun Li[5], Haibin Huang[6], Runhui Zheng[7], Yonghua Li[8], Hui Zeng[9], Robert Peter Gale[10], Tian Ying[11], Jing Guo[3], Zhenshu Xu[12*], Wei Fan[1*] and Tongyu Lin[1,2*]

Abstract

Background Survival prediction accuracy of fluorine-18 fluorodeoxyglucose positron emission tomography/computed tomography (^{18}F-FDG PET/CT) in extra-nodal natural killer/T-cell lymphoma (ENKTL) is controversial. This study aimed to evaluate the prognostic value of ^{18}F-FDG PET/CT parameters including maximum standardized uptake value (SUVmax), total metabolic tumor volume (TMTV) and total lesion glycolysis (TLG), and to develop a new prognostic model for ENKTL.

Methods We analyzed 390 ENKTL patients with comprehensive clinical and survival data. All patients received asparaginase-based chemotherapy with or without radiotherapy, or radiotherapy alone. Metabolic tumor volume (MTV) was calculated using a 41% SUVmax threshold, and TLG was computed as MTV multiplied by the average SUV. Progression-free survival (PFS) and overall survival (OS) were assessed using Kaplan–Meier curves and compared with log-rank tests. Optimal cut-off values were determined using the Youden' index. Cox regression analysis identified significant prognostic factors. A nomogram predicting 1-, 3-, and 5-year survival was developed and validated using the C-index and calibration curves. Statistical significance was set at $p < 0.05$.

Results Of the 390 patients, 262 (67.2%) were included in the training set and 128 (32.8%) in the validation set. ^{18}F-FDG PET-CT parameters with cutoff values of SUVmax > 12.8, TMTV > 16.4 cm^3, and TLG > 137.0, were significantly associated with poorer OS ($p = 0.009$) and PFS ($p = 0.003$). Multivariable Cox regression identified the following as independent predictors of worse OS: age > 60 years (HR = 1.923, 95% CI: 1.001—3.693), presence of B symptoms

†Hua Wang, Demei Feng, Yiwen Mo and Huangming Hong contributed equally to this work.

*Correspondence:
Hua Wang
wanghua@sysucc.org.cn
Zhenshu Xu
zhenshuxu@yahoo.com
Wei Fan
fanwei@sysucc.org.cn
Tongyu Lin
tongyulin@hotmail.com
Full list of author information is available at the end of the article

(HR = 1.861, 1.132—3.059), ECOG score ≥ 2 (HR = 2.076, 1.165—3.699), extranodal involvement ≥ 2 sites (HR = 2.349, 1.384—3.988), bone marrow involvement (HR = 4.884, 2.137—11.163), SUVmax > 12.8 (HR = 2.226, 1.260—3.930), and TMTV > 16.4 cm^3 (HR = 1.854, 1.093—3.147). The new prognostic model achieved a C-index of 0.772 for OS and 0.750 for PFS in the training set, and 0.777 for OS and 0.696 for PFS in the validation set. Area under the curve (AUC) values for 1-, 3-, and 5-year OS were 0.841, 0.804, and 0.767 in the training set, and 0.718, 0.786, and 0.893 in the validation set. Risk stratification divided patients into four groups with significant differences in survival ($p < 0.001$).

Conclusion SUVmax, TMTV, and TLG are independent prognostic factors in ENKTL. Our new model, which integrates ^{18}F-FDG PET/CT metrics with clinical data, enhances survival prediction and may support personalized treatment strategies, though further validation is required.

Keywords Extra-nodal natural killer/T-cell lymphoma(ENKTL), ^{18}F-FDG PET/CT, Total metabolic tumor volume (TMTV), Total lesion glycolysis (TLG), SUVmax

Background

Extra-nodal natural killer/T-cell lymphoma (ENKTL) is a rare subtype of non-Hodgkin lymphoma characterized by Epstein-Barr virus (EBV)-infection and extra-nodal lymph node involvement [1, 2]. Fluorine-18 fluorodeoxyglucose (^{18}F-FDG) positron emission tomography/computed tomography (PET/CT) has become an important tool for staging and monitoring treatment response in lymphomas. ^{18}F-FDG PET/CT offers an advantage over traditional imaging by quantifying metabolic activity.

While ^{18}F-FDG PET/CT is commonly used to estimate progression-free survival (PFS) and overall survival (OS) in ENKTL, the most frequently assessed parameter is the maximum standardized uptake value (SUVmax). However, emerging evidence suggests that parameters reflecting metabolic tumor activity may provide more accurate prognostic information. For instance, small studies in other types of lymphomas have explored the prognostic significance of volume-based metrics such as total metabolic tumor volume (TMTV) and total lesion glycolysis (TLG) [3–5]. Kim et al. demonstrated that higher values for SUVmax, MTV, and TLG were associated with shorter PFS and OS, whereas Pak et al. found no such correlation [6, 7].

In this study, we aimed to evaluate the prognostic value of PET/CT parameters, including SUVmax,TMTV, and TLG, in ENKTL and to develop a new prognostic model to improve survival prediction.

Materials and methods

Patients

This study employed external validation, including 262 newly diagnosed ENKTL patients treated between January 2003 and June 2023 at Sun Yat-sen University Cancer Center as the training set, and 128 patients from eight other independent centers across China during the same period as the validation set. Inclusion criteria include: (1) age > 18 years; (2) ENKTL diagnosed by 2 experienced pathologists with discordances resolved by a third; There was no central review; (3)^{18}F-FDG PET/CT scan before starting therapy; (4) initial therapy with asparagine-based chemotherapy, radiation therapy or both. The diagnosis of ENKTL for all patients was confirmed or reclassified based on the 2016 World Health Organization (WHO) Classification of Lymphoid Neoplasms to ensure consistency across the cohort [8]. Similarly, treatment responses for all patients, including those treated before 2014, were retrospectively assessed using the 2014 Lugano classification to maintain a uniform evaluation framework [9].

^{18}F-FDG PET/CT and other co-variates

Fluorine-18 fluorodeoxyglucose was administered intravenously after confirming normal blood glucose levels were within the normal range (4–7 mmol/L) to ensure accurate PET/CT imaging results [10]. PET/CT scans were done 60 min post-injection using a dedicated scanner (Discovery ST, GE Healthcare, Waukesha, WI, USA or Biograph mCT, Siemens Healthcare, Henkestr, Germany). Continuous emission scanning images from the base of the skull to the proximal thigh, were acquired and images reconstructed using an iterative algorithm that employs ordered subset expectation maximization [11]. PET acquisition was done in 3D mode with 5 min per bed position. CT images were acquired at 140 kV, 150–160 mA, and a 5-mm slice thickness [12].

^{18}F-FDG PET/CT data were evaluated by 2 expert nuclear medicine physicians with discordances resoled by a third. Other co-variates include subject baseline covariates, EBV-infection incidence, disease stage and B symptoms etc. (Table 1). Plasma EBV-DNA was quantified via polymerase chain reaction (qPCR), with positive detection defined as EBV-DNA presence [13].

Table 1 Characteristics of patients in the training and validation cohort

Characteristics	Total ($n=390$)	Training cohort ($n=262$,67.2%)	Validation cohort ($n=128$,32.8%)	*p*
Age > 60 years	64 (16.4)	35 (13.4)	29 (22.7)	0.020
Male sex	253 (64.9)	170 (64.9)	83 (64.8)	0.994
B symptoms	170 (43.6)	117 (44.7)	53 (41.4)	0.543
ECOG ≥ 2	74 (19.0)	43 (16.4)	31 (24.2)	0.065
III- IV stage	116 (29.7)	72 (27.5)	44 (34.4)	0.162
Primary site in other sites	75 (19.2)	57 (21.8)	18 (14.1)	0.070
Local invasion	254 (65.1)	173 (66.0)	81 (63.3)	0.593
Regional lymph node involvement	199 (51.0)	136 (51.9)	63 (49.2)	0.618
Distant lymph node involvement	77 (19.7)	56 (21.4)	21 (16.4)	0.247
Extranodal involvement(s) > = 2	128 (32.8)	87 (33.2)	41 (32.0)	0.817
Bone marrow involvement	33 (8.5)	11 (4.2)	22 (17.2)	< 0.001
Lactic dehydrogenase Elevated	142 (36.4)	85 (32.4)	57 (44.5)	0.020
EBV-DNA				
Positive	252 (61.3)	189 (72.1)	63 (49.2)	0.016
Unknowen	57 (17.6)	12 (4.5)	45 (35.1)	< 0.001
SUVmax > 12.8	204 (52.3)	155 (59.2)	49 (38.3)	< 0.001
TMTV > 16.4 cm^3	201 (51.5)	120 (45.8)	81 (63.3)	0.001
TLG > 137.0	167 (42.8)	119 (45.4)	48 (37.5)	0.138
IPI				0.027
Low risk	253 (64.9)	182 (69.5)	71 (55.5)	
Medium risk	69 (17.7)	41 (15.6)	28 (21.9)	
Medium to high risk	46 (11.8)	24 (9.2)	22 (17.2)	
High risk	22 (5.6)	15 (5.7)	7 (5.5)	
KPI				0.113
Group 1	93 (23.9)	67 (25.6)	26 (20.3)	
Group 2	109 (28.0)	67 (25.6)	42 (32.8)	
Group 3	84 (21.5)	63 (24.1)	21 (16.4)	
Group 4	104 (26.7)	65 (24.8)	39 (30.5)	
PINK				0.548
Low risk	189 (48.5)	132 (50.4)	57 (44.5)	
Medium risk	109 (28.0)	71 (27.1)	38 (29.7)	
High risk	92 (24.0)	59 (22.5)	33 (25.8)	
PINKE				0.080
Low risk	55 (16.5)	15 (18.1)	40 (16.0)	
Medium risk	125 (37.5)	22 (26.5)	103 (41.2)	
High risk	78 (23.4)	21 (25.3)	57 (22.8)	
NRI				0.038
Low risk	65 (16.7)	17 (13.3)	48 (18.3)	
Low to medium risk	71 (18.2)	22 (17.2)	49 (18.7)	
Medium to high risk	93 (23.9)	24 (18.8)	69 (26.3)	
High risk	71 (18.2)	24 (18.8)	47 (17.9)	
Very high risk	90 (23.1)	41 (32.0)	49 (18.7)	

The *p*-value comparing training and validation cohort was calculated via the chi-square test

Abbreviations: *ECOG* Eastern Cooperative Oncology Group performance status, *EBV* Epstein-Barr virus, *SUVmax* maximum standardized uptake value, *TMTV* total metabolic tumor volume, *TLG* total lesion glycolysis, *IPI* International Prognostic Index, *KPI* Korean Prognostic Index, *PINK/PINKE* Prognostic Index for Natural Killer cell lymphoma (E denotes inclusion of EBV-DNA level), *NRI* Nomogram—Revised Risk Index

Image acquisition

Lesions were semi-automatically delineated using a volume of interest (VOI) based on axial, coronal, and sagittal PET/CT images. A cross-sectional circle was placed on each image, covering the lesion in all three planes. The VOI boundaries were manually adjusted to exclude physiological uptake near the lesion. The 41% SUVmax threshold, as recommended by the European Association of Nuclear Medicine, was used to define the VOI [10]. SUVmax and MTV for each lesion were recorded, while TLG was calculated as the product of SUVmean and MTV. These calculations were performed automatically using the Xeleris workstation (GE Medical Systems) [10].

Statistics

Baseline characteristics were compared using the chi-square test. PFS was defined as the time from diagnosis to disease progression, recurrence, death, or last follow-up. OS was defined as the time from diagnosis to death from any cause or last follow-up. For PET/CT parameters (SUVmax, TMTV, and TLG), receiver operating characteristic (ROC) curves were generated using the pROC package (version 1.15.3) in R to determine optimal cutoff values. Univariable and multivariable Cox regression analyses, using the Forward LR method, were conducted to identify independent prognostic factors [4]. Significant variables ($p<0.05$) from univariable analysis were included in the multivariable analysis. A nomogram was constructed to predict 1-, 3-, and 5-year survival rates, assigning weights based on hazard ratios (HR). The nomogram's performance was assessed using the C-index and calibration curves, while net reclassification improvement (NRI) was used to evaluate predictive capability and net benefit. All analyses were repeated 1,000 times using Bootstrap resampling to minimize bias. Risk groups in the modeling set were stratified based on total scores, and survival differences between groups were compared using Kaplan–Meier curves and the log-rank test. DeLong's test was conducted to compare the AUC values between the new model and existing models [14]. Data analysis was performed using R (version 4.0.3) and SPSS (version 25, IBM Corp, Armonk, NY), with statistical significance set at $p<0.05$ [15, 16].

Results

Patient characteristics

In the training set ($n=262$), 35 patients (13.4%) were over 60 years old, compared to 29 (22.7%) in the validation set ($n=128$) ($p=0.020$). In the training set, 170 patients (64.9%) were male, compared to 83 (64.8%) in the validation set ($p=0.994$). Stage III/IV disease was present in 72 patients (27.5%) in the training set and 44 (34.4%) in the validation set ($p=0.150$). Non-nasal primary sites were observed in 57 patients (21.8%) in the training set and 18 (14.1%) in the validation set ($p=0.070$). Bone marrow involvement was significantly more common in the validation set, occurring in 22 patients (17.2%) compared to 11 patients (4.2%) in the training set ($p<0.001$). These results indicate that the baseline characteristics of the two cohorts are largely comparable. Detailed patient characteristics are provided in Table 1.

^{18}F-FDG PET/CT co-variates

The median values for ^{18}F-FDG PET/CT parameters in the training set were: SUVmax = 14.1 (IQR: 10.3–18.6), TMTV = 15.0 cm^3 (IQR: 7.0–34.0), and TLG = 118.4 (IQR: 45.2–262.4). The AUCs for SUVmax, TMTV, and TLG were 0.59, 0.62, and 0.65, respectively, indicating their classification abilities. The optimal cutoff values were 12.8 for SUVmax (sensitivity: 0.73, specificity: 0.46), 16.4 cm^3 for TMTV (sensitivity: 0.64, specificity: 0.61), and 137.0 for TLG (sensitivity: 0.64, specificity: 0.61). Kaplan–Meier survival plots (Fig. 1) revealed significant differences in PFS ($p=0.003$) and OS ($p=0.009$) between patients with low and high SUVmax. For TMTV and TLG, all p-values for both PFS and OS were less than 0.001.

Model construction and validation

Univariate analysis identified all clinical and PET/CT parameters, except for sex ($p=0.910$), as significant predictors ($p<0.05$). These variables were included in the multivariable Cox regression analysis (Table 2), which identified the following predictors of poor OS: age > 60 years (HR = 1.923, 95% CI: 1.001–3.693), presence of B symptoms (HR = 1.861, 95% CI: 1.132–3.059), ECOG ≥ 2 (HR = 2.076, 95% CI: 1.165–3.699), extranodal involvement ≥ 2 sites (HR = 2.349, 95% CI: 1.384–3.988), bone marrow involvement (HR = 4.884, 95% CI: 2.137–11.163), SUVmax > 12.8 (HR = 2.226, 95% CI: 1.260–3.930), and TMTV > 16.4 cm^3 (HR = 1.854, 95% CI: 1.093–3.147). These variables were integrated into a nomogram for predicting 1-, 3-, and 5-year OS in ENKTL patients (Fig. 2). Calibration plots (Fig. 3) showed good agreement between predicted and observed survival probabilities at 1, 3, and 5 years. ROC curves (Fig. 4) indicated AUCs for OS at 1, 3, and 5 years in the training cohort were 0.841, 0.804, and 0.767, respectively, and for PFS, 0.832, 0.778, and 0.754. In the validation cohort, AUCs for OS were 0.718, 0.786, and 0.893, and for PFS, 0.672, 0.695, and 0.822.

Comparison with existing models

The new model outperformed the International Prognostic Index (IPI), Korean Prognostic Index (KPI), Prognostic Index of Natural Killer Lymphoma with or

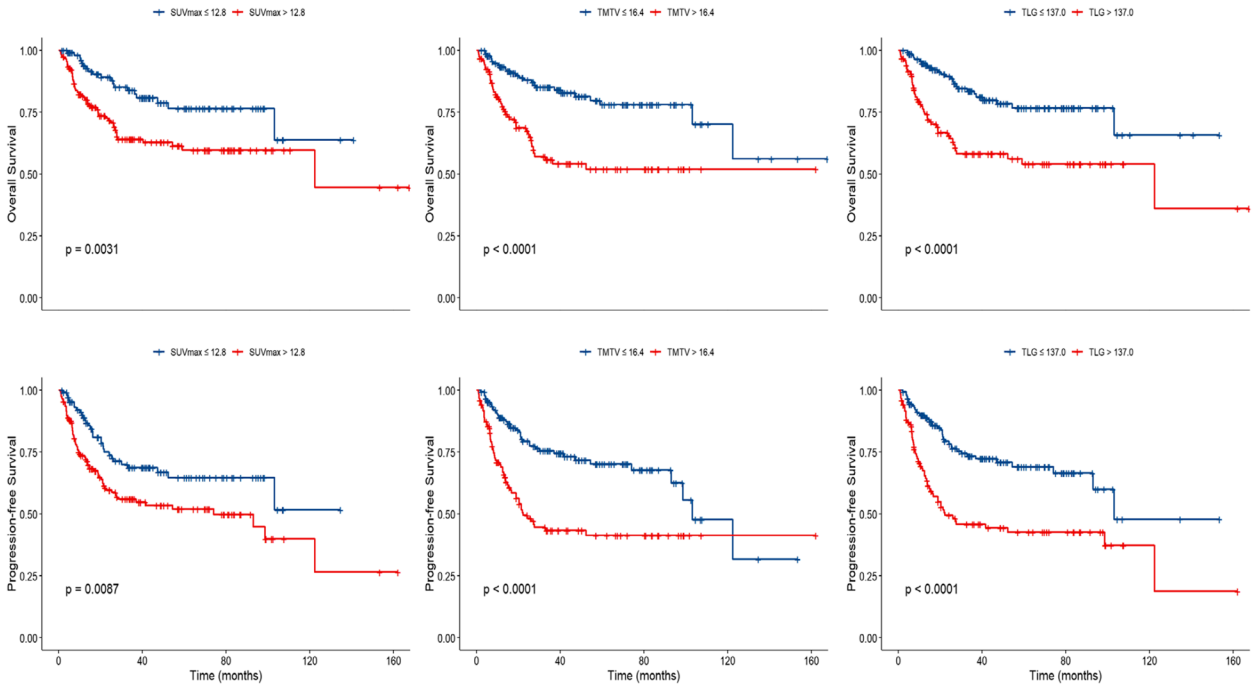

Fig. 1 Kaplan–Meier survival plots based on dichotomized ^{18}F-FDG PET/CT Parameters using cut-off. Abbreviations: SUVmax, maximum standardized uptake value; TMTV, total metabolic tumor volume; TLG, total lesion glycolysis

Table 2 Univariate and multivariate analysis for OS in the training cohort

Characteristics	Univariate analysis		Multivariate analysis	
	HR (95% CI)	*p*-value	HR (95% CI)	*p*-value
Age > 60 years	2.120(1.179—3.812)	0.012	1.923(1.001—3.693)	0.049
B symptoms	2.106(1.301—3.409)	0.002	1.861(1.132—3.059)	0.014
ECOG > = 2	2.895(1.721—4.868)	< 0.001	2.076(1.165—3.699)	0.013
III-IV stage	2.380(1.454—3.897)	0.001	0.569(0.267—1.212)	0.144
Primary site in other sites	2.452(1.509—3.982)	< 0.001	1.422(0.762—2.654)	0.268
Local invasion	2.208(1.261—3.865)	0.006	0.777(0.402—1.502)	0.454
Regional lymph node involvement	3.121(1.832—5.317)	< 0.001	1.662(0.917—3.013)	0.094
Distant lymph node involvement	2.979(1.820—4.876)	< 0.001	0.909(0.438—1.884)	0.797
Extranodal involvement(s) > = 2	3.064(1.903—4.934)	< 0.001	2.349(1.384—3.988)	0.002
Bone marrow involvement	5.768(2.733—12.174)	0.000	4.884(2.137—11.163)	< 0.001
Lactic dehydrogenase Elevated	2.012(1.242—3.260)	0.005	1.174(0.690—1.997)	0.554
SUVmax > 12.8	2.172(1.282—3.681)	0.004	2.226(1.260—3.930)	0.006
TMTV > 16.4 cm^3	2.913(1.779—4.770)	< 0.001	1.854(1.093—3.147)	0.022
TLG > 137.0	2.745(1.682—4.480)	< 0.001	0.937(0.439—2.000)	0.866

Abbreviations: *OS* overall survival, *HR* hazard ratio, *95% CI* 95% confidence interval

without EBV DNA (PINK/PINK-E), and the Nomogram—Revised Risk Index (NRI) models in terms of both C-index and AUC values for predicting OS and PFS at 1, 3, and 5 years. For the training set, in 1000 bootstrap samples, the new model has the highest Harrell's C-index for OS (0.772, 95% CI: 0.730—0.837) and PFS (0.750, 95% CI: 0.711—0.780), outperforming the IPI (OS: 0.686, PFS: 0.689), KPI (OS: 0.700, PFS: 0.703), PINK (OS: 0.661, PFS: 0.664), and NRI(OS: 0.717, PFS: 0.734) models (Table 3). Similarly, the new model shows higher AUC values across 1, 3, and 5 years in the training set, with OS (1-year: 0.841, 3-year: 0.804, 5-year: 0.767) and PFS

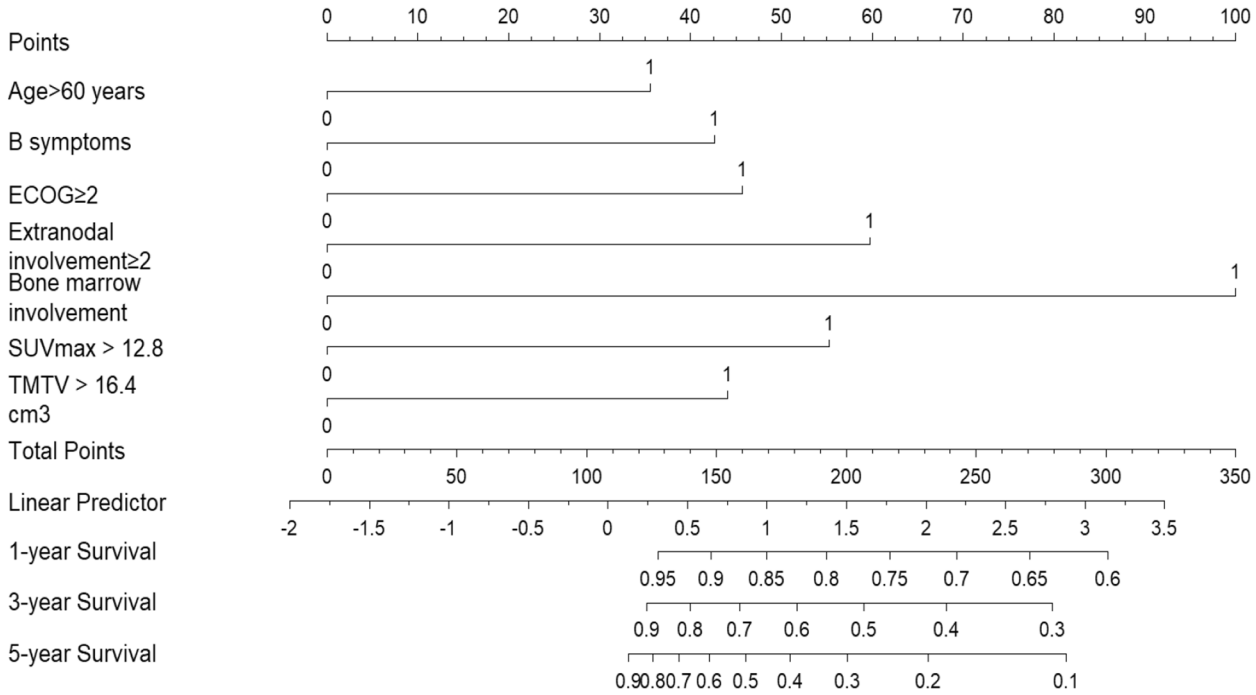

Fig. 2 Nomogram for predicting 1-year, 3-year, and 5-year overall survival rates in training cohort

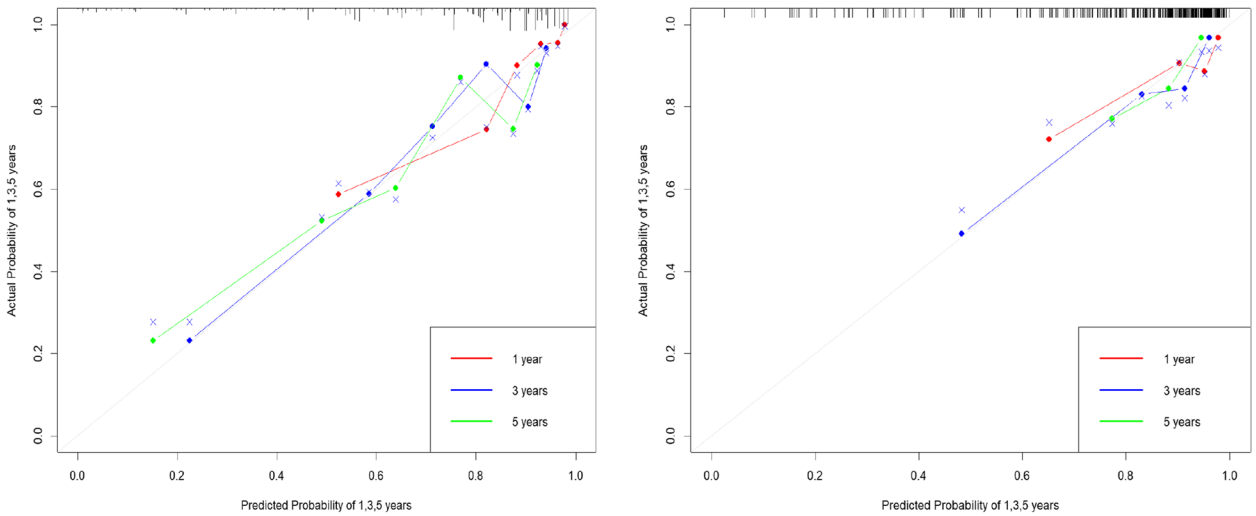

Fig. 3 Calibration plots for 1-year, 3-year, and 5-year overall survival

(1-year: 0.832, 3-year: 0.778, 5-year: 0.754). In the validation set, the new model also excels with a C-index for OS of 0.777 (95% CI: 0.661—0.873) and for PFS of 0.696 (95% CI: 0.600—0.787), surpassing the IPI (OS: 0.731, PFS: 0.709), KPI (OS: 0.745, PFS: 0.687), PINK (OS: 0.702, PFS: 0.673),and NRI (OS: 0.726, PFS:0.723) models. Furthermore, it has consistently higher AUCs for OS (1-year: 0.718, 3-year: 0.766, 5-year: 0.893) and PFS (1-year: 0.672, 3-year: 0.695, 5-year: 0.822), highlighting its improved prognostic capabilities (Figure S1 and S2).

To further validate these results, DeLong's test was applied to compare the AUC values of the new model with those of existing models in the full dataset. For OS, the new model showed significantly higher AUC values compared to the IPI ($p<0.001$), KPI ($p=0.011$), PINK ($p=0.001$), and NRI ($p=0.002$) models. For PFS,

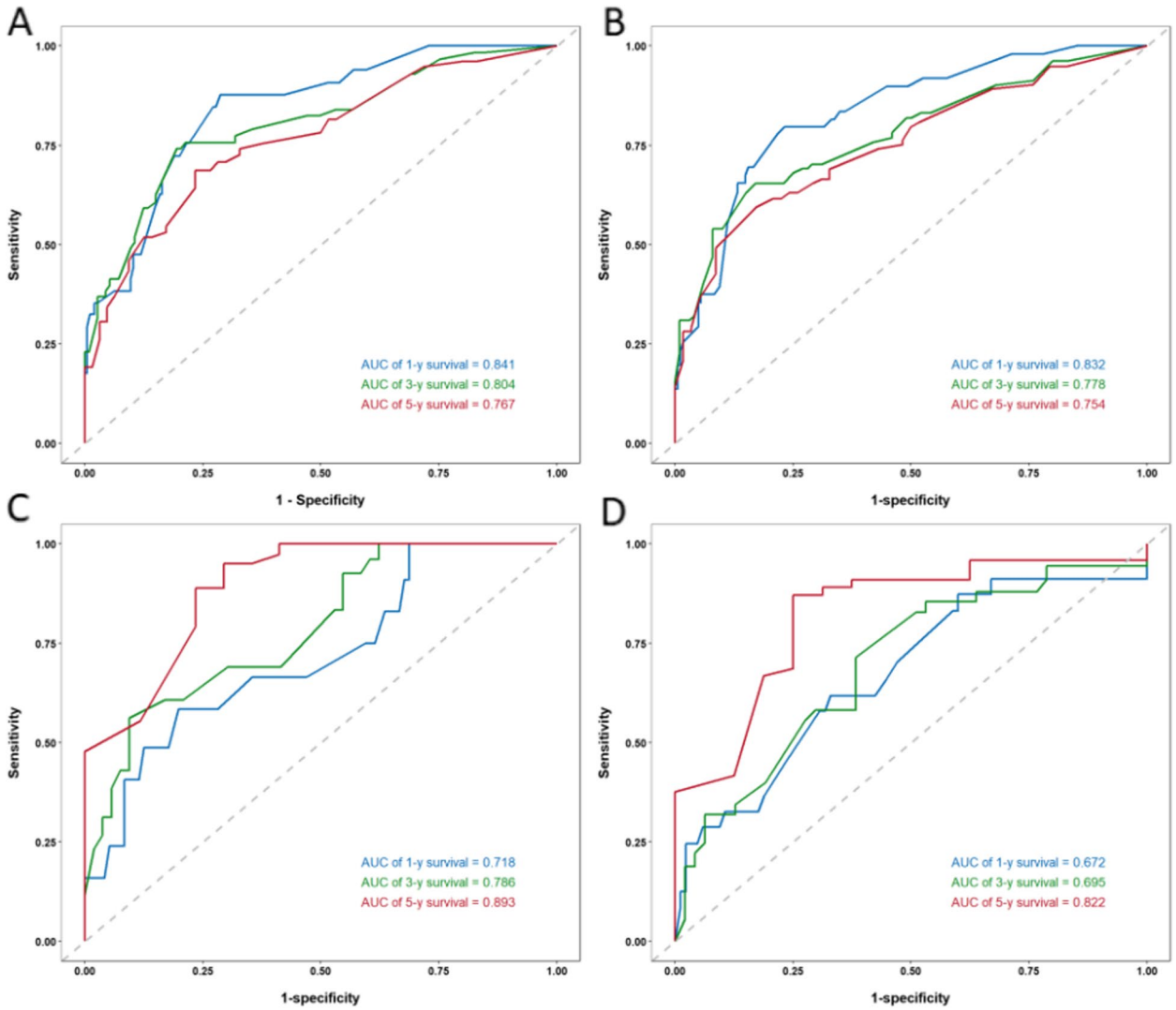

Fig. 4 **A** and **B** indicate the ROC curves for OS and PFS in the training cohort, **C** and **D** indicate the ROC curves for OS and PFS in the validation cohort. Abbreviations: AUC: area under the curve; ROC: receiver operating characteristic; OS: overall survival; PFS: progression-free survival

Table 3 The C-index values of models for OS and PFS

Model	Training set		Validation set	
	OS	PFS	OS	PFS
IPI	0.686 (0.617—0.754)	0.689 (0.631—0.744)	0.732 (0.628—0.829)	0.696 (0.600—0.785)
KPI	0.700 (0.636—0.764)	0.703 (0.652—0.754)	0.745 (0.633—0.844)	0.692 (0.592—0.772)
PINK	0.661 (0.580—0.731)	0.664 (0.605—0.718)	0.701 (0.595—0.801)	0.660 (0.560—0.759)
NRI	0.718 (0.654—0.778)	0.734 (0.683—0.784)	0.737 (0.621—0.844)	0.721 (0.631—0.809)
New model	0.772 (0.730—0.837)	0.750 (0.711—0.780)	0.777 (0.661—0.833)	0.696 (0.600—0.787)

significant differences were observed between the new model and the IPI ($p=0.004$) and PINK ($p=0.014$) models.

Construction and validation of the risk stratification model

Based on the hazard ratio (HR) estimates, bone marrow involvement (HR = 4.884) was assigned a weight of 2, while age > 60 years, B symptoms, ECOG ≥ 2,

extranodal involvement ≥ 2 sites, SUVmax > 12.8, and MTV > 16.4 cm^3 were assigned a weight of 1. Patients in the training cohort were stratified into four risk groups: (1) low-risk (Score 0–1, $n = 96$, 36.6%), (2) low-intermediate-risk (Score 2–3, $n = 120$, 45.8%), (3) intermediate-high-risk (Score 4–5, $n = 39$, 14.9%), and (4) high-risk (Score 7, $n = 27$, 2.7%). Kaplan–Meier survival analysis showed significant differences in OS and PFS among the four groups (Fig. 5A and B). In the validation cohort, Group 2 tended to have worse OS compared to Group 1 ($p = 0.174$), while Groups 3 and 4 showed significant differences ($p < 0.001$) (Fig. 5C and D).

Impact of treatments across risk stratifications

To ensure sufficient data for all three treatment modalities within each risk stratum, we combined the training and validation sets for analysis. Figure 6 illustrates the impact of different treatment strategies on OS and PFS across various risk strata. In the low-risk group, no significant differences in OS or PFS were observed among radiotherapy (RT), chemotherapy (CT), and combined chemoradiotherapy (CRT) ($p > 0.05$). In the intermediate-low risk group, CRT significantly improved OS compared to RT ($p = 0.012$) and CT ($p = 0.011$), and PFS compared to CT ($p = 0.005$), with no significant differences between RT and CT or RT and CRT for PFS ($p > 0.05$). In the intermediate-high risk group, CRT demonstrated significantly

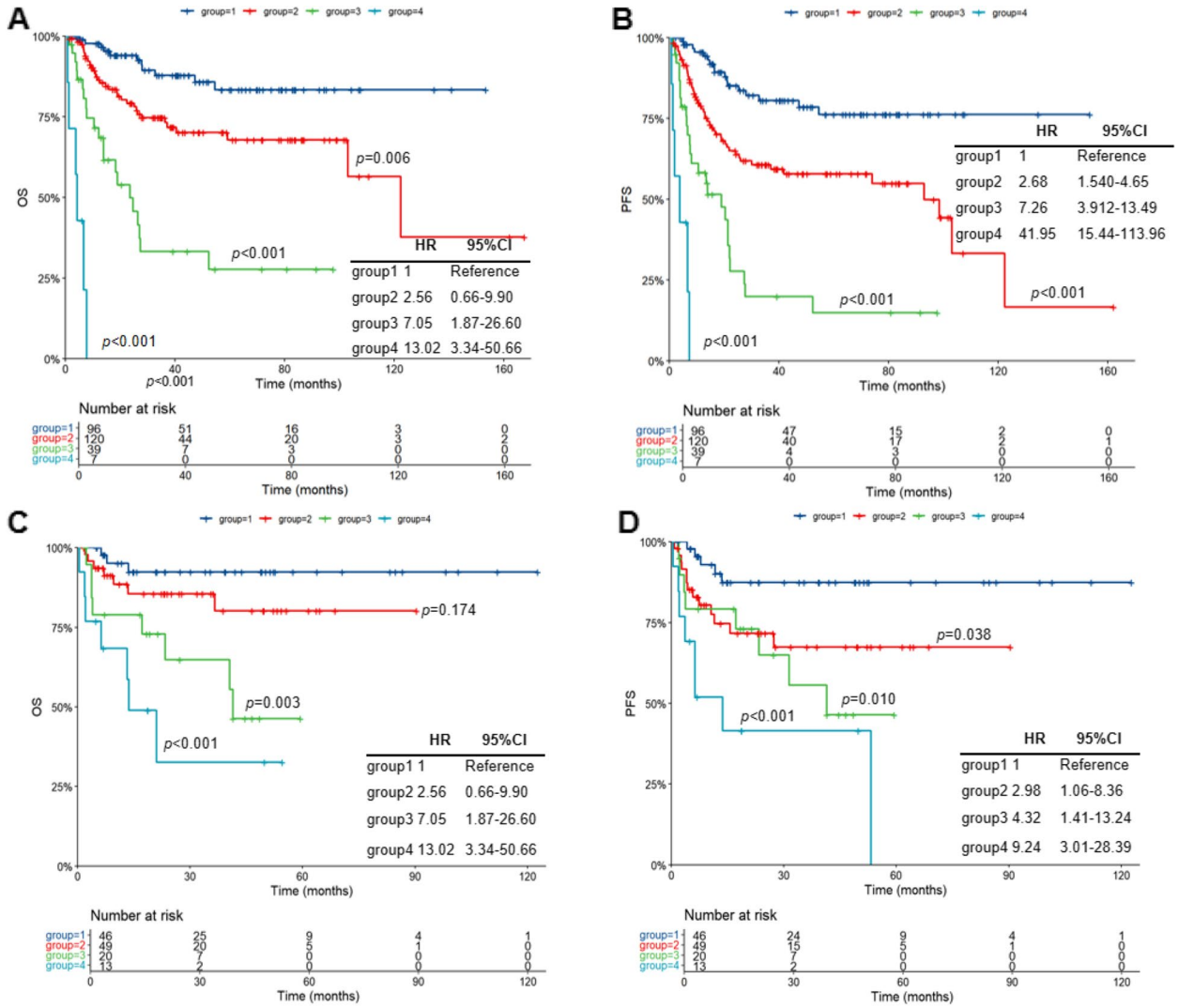

Fig. 5 **A** and **B** indicate overall and progression-free survival according to new model in the validation cohort, and **C** and **D** indicate overall and progression-free survival according to new model in the validation cohort. Abbreviations: OS, overall survival; HR, hazard ratio; 95% CI, 95% confidence interval

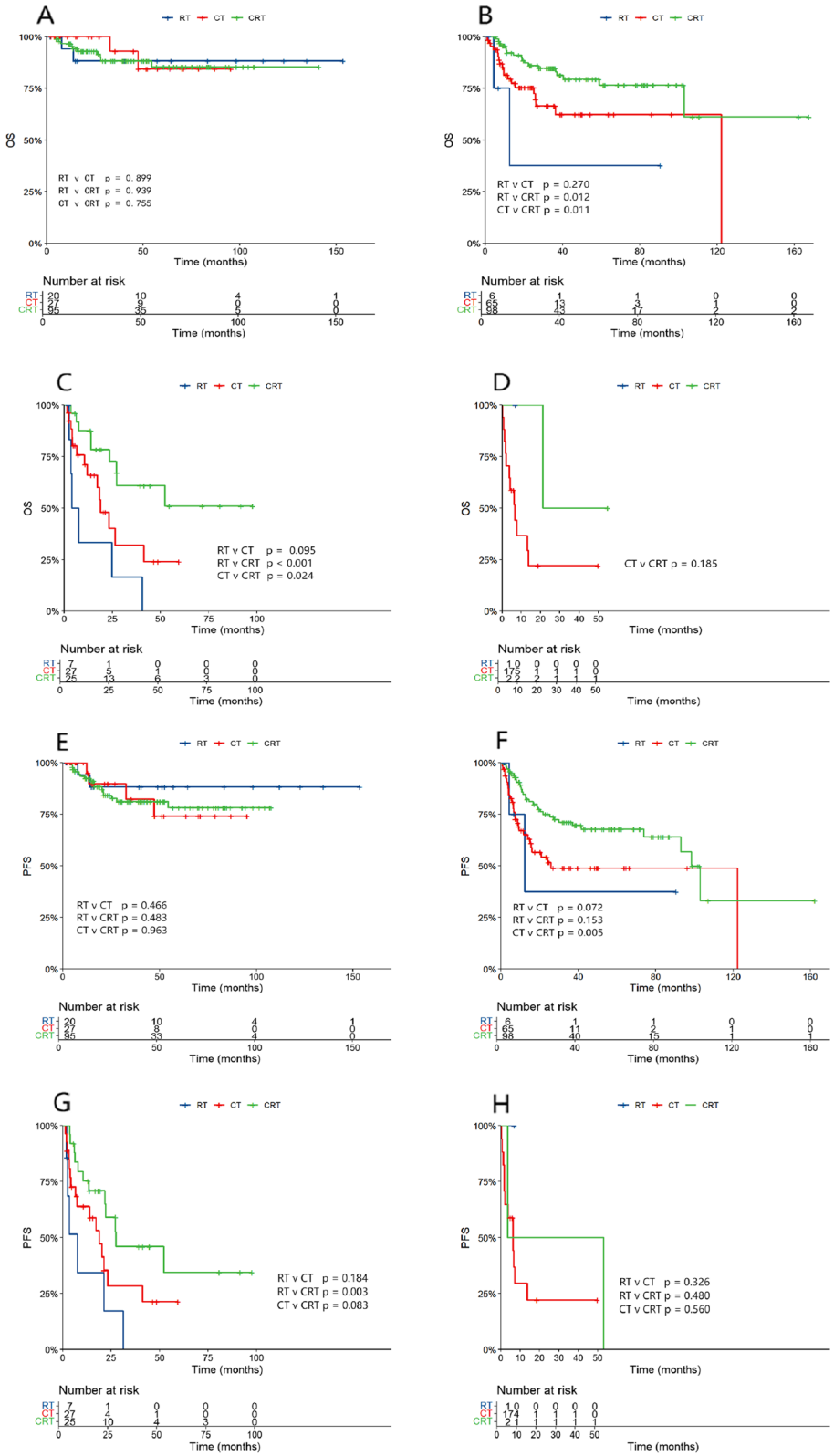

Fig. 6 Kaplan–Meier curves for OS and PFS by treatment modality across risk groups based on the new model. **A**–**D** K-M curves for OS in the low-risk (**A**), intermediate-low risk (**B**), intermediate-high risk (**C**), and high-risk (**D**) groups by treatment modality; **E**–**H** K-M curves for PFS in the low-risk (**E**), intermediate-low risk (**F**), intermediate-high risk (**G**), and high-risk (**H**) groups by treatment modality. Abbreviations: OS, overall survival; PFS, progression-free survival; RT, radiotherapy; CT, chemotherapy; CRT, combined chemoradiotherapy

better OS outcomes versus RT ($p<0.001$) and CT ($p=0.024$), and superior PFS outcomes compared to RT ($p=0.003$), but no significant differences were observed between RT and CT or CT and CRT for PFS ($p>0.05$). In the high-risk group, CRT showed a non-significant trend toward better OS than CT alone ($p=0.185$), with no significant differences in PFS among treatments ($p>0.05$).

Discussion

Although extensive data support the prognostic value of ^{18}F-FDG PET/CT parameters in various lymphomas, including Hodgkin lymphoma, diffuse large B-cell lymphoma, follicular lymphoma, and peripheral T-cell lymphoma, there are limited data for ENKTL [17–19]. SUVmax reflects the peak uptake at one site, while MTV quantifies tumor volume, and TLG captures both tumor volume and metabolic activity, offering a comprehensive picture of tumor burden [20]. Most studies focused on SUVmax. Our data findings suggest ^{18}F-FDG PET/CT baseline metabolic tumour volume and total lesion glycolysis correlate with PFS and OS and developed a new prognostic model in ENKTL.

Several studies have reported divergent prognostic implications of MTV and TLG in lymphomas. Li et al. demonstrated a strong association between high SUVmax values and worse PFS and OS in 171 newly diagnosed ENKTL patients [21]. Chang et al. identified high TLG values as predictors of worse PFS and OS in 52 newly diagnosed ENKTL patients, noting high SUVmax but not MTV as predictive of poor PFS [22]. Kim et al. reported that high MTV was the strongest predictor of PFS and OS in 20 newly diagnosed ENKTL patients, with SUVmax and TLG also significantly correlated with PFS [7]. These authors found that SUVmax, MTV, and TLG independently predicted PFS and OS in univariable analyses. The discrepancies between these studies likely stem from different methods used to define the VOI, resulting in varying cutoff values and the small sample sizes in some cohorts.

Multiple prognostic models for ENKTL have been proposed, including the IPI, KPI, PINK/PINK-E, and the NRI. The IPI tends to predict better outcomes for low-risk patients, but its uneven distribution across risk categories, with approximately 80% of patients classified as low-risk, may underestimate disease aggressiveness in some individuals. The KPI offers greater accuracy but is limited to nasal NKTL [23–25]. The NRI scoring system, while incorporating useful risk factors, was developed based on a cohort where 64% of patients received CHOP (cyclophosphamide, doxorubicin, vincristine, and prednisolone) or similar therapies, which are now considered suboptimal for ENKTL [26, 27].

We developed a new prognostic model that incorporates key clinical and PET/CT parameters, including age > 60 years, presence of B symptoms, ECOG score ≥ 2, extranodal involvement ≥ 2 sites, SUVmax > 12.8, and TMTV > 16.4 cm^3. This model demonstrated superior predictive accuracy for both OS and PFS compared to existing models, with C-statistics of 0.722 for OS and 0.750 for PFS in the training set, and 0.777 for OS and 0.696 for PFS in the validation set.

The proposed risk stratification model offers insights into optimizing treatment strategies for ENKTL patients but requires cautious interpretation. For low-risk patients, the lack of significant differences in OS or PFS among RT, CT, and CRT suggests that intensive combination therapies may not be necessary, potentially sparing these patients from unnecessary toxicity. In intermediate—low risk and intermediate—high risk groups, CRT showed improved survival outcomes compared to RT or CT, indicating its potential as a preferred approach. In the high-risk group, the non-significant trend toward better OS with CRT compared to CT alone, coupled with no observable differences in PFS among treatments, highlights the challenges in managing this population, such as hematopoietic stem cell transplantation (HSCT), immune checkpoint inhibitors, or CAR-T cell therapy, may offer potential benefits and warrant further investigation in clinical trials [28, 29].

Our study advances previous research by integrating SUVmax, TMTV, and TLG with clinical factors to develop a robust prognostic model that stratifies ENKTL patients into four risk groups. Our model offers a practical framework for personalized treatment, enabling therapy de-escalation for low-risk patients and novel strategies for high-risk cases. The use of a larger multicenter cohort and rigorous validation enhances its reliability and clinical applicability, bridging gaps in existing literature and providing actionable insights for improved patient outcomes.

Despite the promising performance of our model, this study has several limitations. First, technical variability in measuring PET/CT parameters across different centers may affect the consistency of the data. Additionally, treatment protocols were not fully standardized among the centers, which could have introduced variability in patient management. Although our sample size is relatively large, it may still limit the external generalizability of the results. Finally, the retrospective nature of the study may introduce bias, underscoring the need for prospective studies to validate our findings.

In summary, we validated the independent prognostic significance of SUVmax, TMTV, and TLG in ENKTL patients and developed a nomogram that incorporates these ^{18}F-FDG PET/CT parameters with

clinical factors, demonstrating improved accuracy in predicting survival. While our model has been externally validated, further prospective studies are necessary to confirm its prognostic utility and applicability in broader clinical settings.

Supplementary Information

The online version contains supplementary material available at https://doi.org/10.1186/s12885-025-13725-9.

Supplementary Material 1.

Authors' contributions

HW, ZSX, YWM, HMH, WF, TYL and TY were responsible for concept and design; WH, DMF were responsible for manuscript preparation and manuscript editing; YYH, LH, XLW, YJL, HBH, RHZ, YHL, HZ, JG were responsible for the data acquisition and literature search; HW and RPG contributed to revised the manuscript.

Funding

HW is supported by National Natural Science Foundation of China grant 81700148 and Natural Science Foundation of Guangdong Province grant 2021A1515010093 and 2023A1515011862.

Data availability

No datasets were generated or analysed during the current study. The data are available from the corresponding author upon reasonable request.

Declarations

Ethics approval and consent to participate

This study received approval from the Institutional Ethical Review Board of Sun Yat-Sen University Cancer Center, which also waived the requirement for informed consent. The study's methodology was based on the International Conference on Harmonization's Good Clinical Practice standards and the 1964 Helsinki Declaration, including its later revisions.

Consent for publication

Not applicable.

Competing interests

The authors declare no competing interests.

Author details

[1]State Key Laboratory of Oncology in South China, Guangdong Provincial Clinical Research Center for Cancer, Sun Yat-Sen University Cancer Center, Guangzhou 510060, P. R. China. [2]Sichuan Caner Hospital & Institute / Sichuan Cancer Prevention and Control Center / Affiliated Cancer Hospital of University of Electronic Science and Technology of China, Chengdu, Sichuan 610041, China. [3]The Affiliated Hospital of Southwest Medical University, Luzhou, Sichuan 646501, China. [4]Department of Hematology, Nanfang Hospital, Southern Medical University, Guangzhou 510515, China. [5]Department of Lymphoma & Hematology, Hunan Cancer Hospital, Changsha, Hunan 410013, China. [6]The Third Affiliated Hospital of Southern Medical University, Guangzhou, Guangdong 510070, China. [7]Department of Hematology, Fifth Affiliated Hospital, Guangzhou Medical University, Guangzhou, Guangdong 510735, China. [8]Department of Onset, Guangzhou Southern Theater Command General Hospital, Guangzhou 510010, China. [9]The First Affiliated Hospital of Jinan University, Guangzhou, Guangdong 510632, China. [10]Haematology Research Centre, Department of Immunology and Inflammation, Imperial College London, London, UK. [11]Department of Nuclear Medicine, Nanfang Hospital, Southern Medical University, 1838 Guangzhou Avenue North, Guangzhou 510515, China. [12]Department of Hematology, Union Hospital, Fujian Medical University, Fujian Institute of Hematology, Fuzhou, Fujian 350000, China.

Received: 13 November 2024 Accepted: 12 February 2025
Published online: 03 March 2025

References

1. de Leval L, Feldman AL, Pileri S, Nakamura S, Gaulard P. Extranodal T- and NK-cell lymphomas. Virchows Arch. 2023;482(1):245–64. https://doi.org/10.1007/s00428-022-03434-0.
2. Coenen HH, Gee AD, Adam M, et al. Consensus nomenclature rules for radiopharmaceutical chemistry - setting the record straight. Nucl Med Biol. 2017;55:v–xi. https://doi.org/10.1016/j.nucmedbio.2017.09.004.
3. Zhang YY, Song L, Zhao MX, Hu K. A better prediction of progression-free survival in diffuse large B-cell lymphoma by a prognostic model consisting of baseline TLG and %ΔSUVmax. Cancer Med. 2019;8(11):5137–47. https://doi.org/10.1002/cam4.2284.
4. Feng X, Wen X, Li L, et al. Baseline total metabolic tumor volume and total lesion glycolysis measured on 18F-FDG PET-CT predict outcomes in T-cell lymphoblastic lymphoma. Cancer Res Treat. 2021;53(3):837–46. https://doi.org/10.4143/crt.2020.123.
5. Liang JH, Zhang YP, Xia J, et al. Prognostic value of baseline and interim total metabolic tumor volume and total lesion glycolysis measured on 18F-FDG PET-CT in patients with follicular lymphoma. Cancer Res Treat. 2019;51(4):1479–87. https://doi.org/10.4143/crt.2018.649.
6. Pak K, Kim BS, Kim K, et al. Prognostic significance of standardized uptake value on F18-FDG PET/CT in patients with extranodal nasal type NK/T cell lymphoma: a multicenter, retrospective analysis. Am J Otolaryngol. 2018;39(1):1–5. https://doi.org/10.1016/j.amjoto.2017.10.009.
7. Kim CY, Hong CM, Kim DH, et al. Prognostic value of whole-body metabolic tumour volume and total lesion glycolysis measured on ^{18}F-FDG PET/CT in patients with extranodal NK/T-cell lymphoma. Eur J Nucl Med Mol Imaging. 2013;40(9):1321–9. https://doi.org/10.1007/s00259-013-2443-6.
8. Swerdlow SH, Campo E, Pileri SA, et al. The 2016 revision of the World Health Organization classification of lymphoid neoplasms. Blood. 2016;127(20):2375–90. https://doi.org/10.1182/blood-2016-01-643569.
9. Cheson BD, Fisher RI, Barrington SF, et al. Recommendations for initial evaluation, staging, and response assessment of Hodgkin and non-Hodgkin lymphoma: the Lugano classification. J Clin Oncol. 2014;32(27):3059–68. https://doi.org/10.1200/JCO.2013.54.8800.
10. Boellaard R, Delgado-Bolton R, Oyen WJG, et al. FDG PET/CT: EANM procedure guidelines for tumour imaging: version 2.0. Eur J Nucl Med Mol Imaging. 2015;42(2):328–54. https://doi.org/10.1007/s00259-014-2961-x.
11. Li M, Yao H, Zhang P, et al. Development and validation of a [18F]FDG PET/CT-based radiomics nomogram to predict the prognostic risk of pretreatment diffuse large B cell lymphoma patients. Eur Radiol. 2023;33(5):3354–65. https://doi.org/10.1007/s00330-022-09301-5.
12. Wei WX, Huang JJ, Li WY, et al. Prognostic values of interim and post-therapy 18F-FDG PET/CT scanning in adult patients with Burkitt's lymphoma. Chin J Cancer. 2015;34:59. https://doi.org/10.1186/s40880-015-0057-z.
13. Suwiwat S, Pradutkanchana J, Ishida T, Mitarnun W. Quantitative analysis of cell-free Epstein-Barr virus DNA in the plasma of patients with peripheral T-cell and NK-cell lymphomas and peripheral T-cell proliferative diseases. J Clin Virol. 2007;40(4):277–83. https://doi.org/10.1016/j.jcv.2007.08.013.
14. Demler OV, Pencina MJ, D'Agostino RB. Misuse of DeLong test to compare AUCs for nested models. Stat Med. 2012;31(23):2577–87. https://doi.org/10.1002/sim.5328.
15. Wang H, Fu BB, Wuxiao ZJ, et al. A prognostic survival nomogram for persons with extra-nodal natural killer-/T-cell lymphoma. Leukemia. 2022;36(11):2724–8. https://doi.org/10.1038/s41375-022-01679-x.
16. Yang Y, Zhang YJ, Zhu Y, et al. Prognostic nomogram for overall survival in previously untreated patients with extranodal NK/T-cell lymphoma, nasal-type: a multicenter study. Leukemia. 2015;29(7):1571–7. https://doi.org/10.1038/leu.2015.44.
17. Frood R, Burton C, Tsoumpas C, et al. Baseline PET/CT imaging parameters for prediction of treatment outcome in Hodgkin and diffuse large B cell lymphoma: a systematic review. Eur J Nucl Med Mol Imaging. 2021;48(10):3198–220. https://doi.org/10.1007/s00259-021-05233-2.
18. Kitadate A, Narita K, Fukumoto K, et al. Baseline total lesion glycolysis combined with interim positron emission tomography-computed

tomography is a robust predictor of outcome in patients with peripheral T-cell lymphoma. Cancer Med. 2020;9(15):5509–18. https://doi.org/10.1002/cam4.3226.
19. Li H, Wang M, Zhang Y, et al. Prediction of prognosis and pathologic grade in follicular lymphoma using (18)F-FDG PET/CT. Front Oncol. 2022;12:943151. https://doi.org/10.3389/fonc.2022.943151.
20. Cheson BD. PET/CT in lymphoma: current overview and future directions. Semin Nucl Med. 2018;48(1):76–81. https://doi.org/10.1053/j.semnuclmed.2017.09.007.
21. Li H, Shao G, Zhang Y, et al. Nomograms based on SUVmax of 18F-FDG PET/CT and cliewly diagnosed extranodal natural killer/T-cell lymphomnical parameters for predicting progression-free and overall survival in patients with na. Cancer Imaging. 2021;21(1):9. https://doi.org/10.1186/s40644-020-00379-y.
22. Chang Y, Fu X, Sun Z, et al. Utility of baseline, interim and end-of-treatment 18F-FDG PET/CT in extranodal natural killer/T-cell lymphoma patients treated with L-asparaginase/pegaspargase. Sci Rep. 2017;7:41057. https://doi.org/10.1038/srep41057.
23. Lee J, Suh C, Park YH, et al. Extranodal natural killer T-cell lymphoma, nasal-type: a prognostic model from a retrospective multicenter study. J Clin Oncol. 2006;24(4):612–8. https://doi.org/10.1200/JCO.2005.04.1384.
24. Huang JJ, Zhu YJ, Xia Y, et al. A novel prognostic model for extranodal natural killer/T-cell lymphoma. Med Oncol. 2012;29(3):2183–90. https://doi.org/10.1007/s12032-011-0030-x.
25. International Non-Hodgkin's Lymphoma Prognostic Factors Project. A predictive model for aggressive non-Hodgkin's lymphoma. N Engl J Med. 1993;329(14):987–94. https://doi.org/10.1056/NEJM199309303291402.
26. Jeong SH. Extranodal NK/T cell lymphoma. Blood Res. 2020;55(S1):S63–71. https://doi.org/10.5045/br.2020.S011.
27. Tse E, Kwong YL. Diagnosis and management of extranodal NK/T cell lymphoma nasal type. Expert Rev Hematol. 2016;9(9):861–71. https://doi.org/10.1080/17474086.2016.1206465.
28. Zhao WL, Cai MC, Zhong HJ. How I diagnose and treat NK/T cell lymphoma. Zhonghua Xue Ye Xue Za Zhi. 2020;41(6):446–50. https://doi.org/10.3760/cma.j.issn.0253-2727.2020.06.002.
29. Tian XP, Cao Y, Cai J, et al. Novel target and treatment agents for natural killer/T-cell lymphoma. J Hematol Oncol. 2023;16(1):78. https://doi.org/10.1186/s13045-023-01483-9.

Publisher's Note